Dynamic and environmental study of a mid-infrared wavelength channel for a horizontal telecom link

Chloé Sauvage, Clélia Robert, Béatrice Sorrente, Frédéric Grillot, Didier Erasme

Dynamic and environmental study of a mid-infrared wavelength channel for a horizontal telecom link

Chloé Sauvage [1,2], Clélia Robert [1], Béatrice Sorrente [1], Fréderic Grillot [2], and Didier Erasme [2]

[1] DOTA, ONERA, Université Paris Saclay, 92320 Chatillon - France
[2] LTCI, Télécom Paris, Institut Polytechnique de Paris, 91120 Palaiseau - France

ABSTRACT

This study characterizes a horizontal atmospheric telecom channel in terms of evolution time of the intensity and the phase of the electromagnetic field received. The channel temporal characterization comes from a turbulence data base recorded during a C_n^2 profiler experiment (SCINDAR). The coherence times of the intensity and phase for an overcast and unclear sky are computed, these values bring information on the bit rate achievable and the speed of an adaptive optics system.

Keywords: Free space optical communication, infrared transmittance, coherence time, wave-front sensing

1. INTRODUCTION : CONTEXT OF THE FREE SPACE OPTICS (FSO)

The FSO is a booming technology, having a lot of advantages such as a faster deployment than the optical fiber network, no spectrum regulation yet and a directional beam then less hackable than radio frequencies [1]. However FSO suffers from the reduction of communication's performance caused by the decrease of atmospheric transmittance, due to fog or particles [2]. In addition, the turbulence effects (beam wander and scintillation leading to signal fadings) [3] may impact the Bit Error Rate (BER) of the optical communication if no mitigation techniques such as adaptive optics (AO) or data interleaving and coding are considered.

The purpose of this study is to characterize a horizontal atmospheric telecom channel in terms of evolution time. In a previous study [4] we investigated the increase of availability of an urban FSO under any weather along a year, especially in case of low visibility that happens in winter. In fact several atmospheric parameters such as aerosols composition, size distribution or weather phenomena (like rain, fog, snow,...) impact the atmospheric transmission of a laser beam. The wavelength is a parameter that can be chosen wisely and controlled in order to increase the transmittance rate. We compared in [4] the pros and the cons of the 4 μm and 1.55 μm, with the help of our radiative transfer software MATISSE [5] to compute the transmittance rate for two weather cases, one with fog and the other without fog, and for a 4 km-long horizontal path. Our main conclusion is that using 4 μm to support the optical communication is a preferred solution in particularly in the case of fog.

This paper is organized as follows : Section 2 describes channel characterization by SCINtillation Detection And Ranging (SCINDAR) experiment, and the coherence times of the intensity and phase of the electromagnetic field received are derived and discussed. Section 3 sums up conclusions and prospects.

2. CHARACTERIZATION OF THE CHANNEL WITH THE SCINDAR

2.1 Measurement method

The SCINDAR experiment [6] uses an infrared Shack-Hartmann wave-front sensor (λ = 3.4 to 4.2 μm) which observes two halogen lamps 1 m-apart and that are located at 4.2 km of the receiver. On average the horizontal line of sight is about 40 m above ground. A 5×5 array of sub-apertures, 20 of which are effectively operative, samples the wave-front at a frequency of 142 Hz. The size of sub-aperture is 7 cm and the diameter of the telescope $D_{telescope}$ is 35 cm. Thus 2×20 = 40 sub-channels, remotly sensed by the 20 sub-apertures imaging the 2 sources, are characterized in form of temporal intensity and wave-front slopes series. Practically the SCINDAR

For more informations send correspondence to C.Sauvage (chloe.sauvage@onera.fr) or C.Robert (clelia.robert@onera.fr)

experiment gathers intensity and turbulent phase in a big data base for several weather conditions and several hours. A distributed C_n^2 profile along the line of sight can also be computed with these data [6]. The C_n^2 represents the structure parameter of the refractive index that quantifies the turbulence strength locally.

2.2 Coherence time of the intensity

The long-term intensity series which had been recorded by the SCINDAR are analyzed in order to study the coherence time of the intensity Δt. The temporal evolution of the channel is to be compared to the bit rate which we are aimed for the FSO link, around few Gbits/s. For instance the bit rate value of Pang and al. [7] is 3 Gbit/s for a direct modulation with a Quantum Cascade Laser. The intensity coherence time Δt is determined for each sub channels of the SCINDAR and at each minute of the temporal series. The coherence time of the intensity Δt corresponds to the width at half maximum of the normalized autocorelation of intensity $\Gamma_{i_{norm}}(t)$ and it can be computed from equation 1 and 2:

$$\Gamma_i(t) = \sum_{n=1}^{nb\ sample} [i_n(t) - < i >]\ [i_n(t-\tau) - < i >]\ , \tag{1}$$

where $\Gamma_i(t)$ is the autocorrelation of intensity, *nb sample* is the number of samples in 60 seconds, here 8520, $< i >$ the average intensity over the 1 min slot, $i_n(t)$ the value of the intensity for the sample n and τ the shift between two samples, equals to $\frac{1}{142}$ s. Then we normalize this result :

$$\Gamma_{i_{norm}}(t) = \frac{\Gamma_i(t)}{max(\Gamma_i(t))}\ . \tag{2}$$

The coherence time of the intensity Δt is the full width at half maximum of $\Gamma_{i_{norm}}(t)$.

Two midday recordings performed in autumn are investigated. The first one corresponds to a 4 hour slot on October 19$^{\text{th}}$, 2015, when the sky was overcast and the visibilities ranging between 6 km and 12 km. During this period the wind $|\vec{v_0}|$ was low, 2.5 m/s in average, and perpendicular to the line of sight. The second period was recorded on the October 30$^{\text{th}}$, 2015, during 5 hours. The sky was partly cloudy with a lots of sunny spells, a better visibility from 16 km to 40 km, and the wind speed was 3.1 m/s in average, parallel to the sight line.

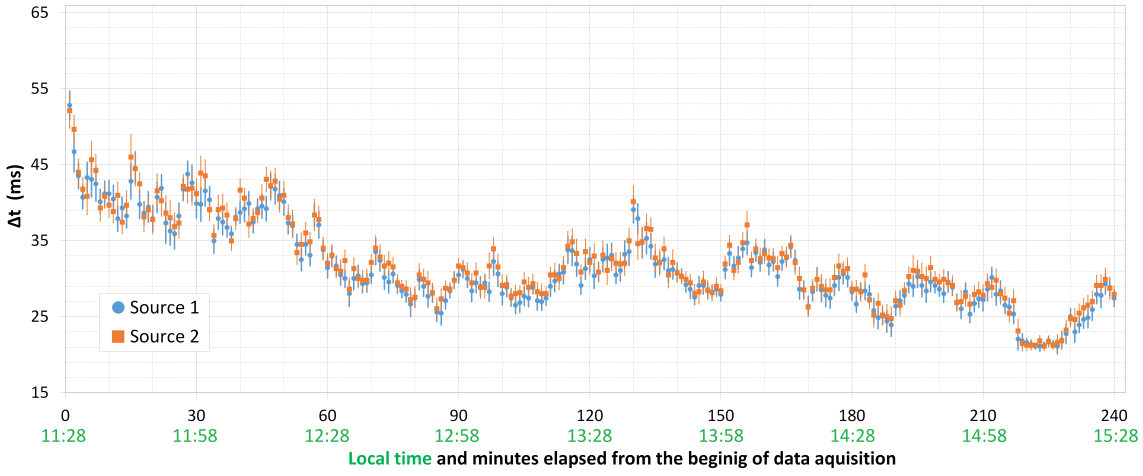

Figure 1. Temporal evolution of the coherence time (Δt) for each source with its standard deviation (October 19$^{\text{th}}$, 2015).

Figures 1 and 2 show the evolution of the averaged coherence time (Δt) for each source. The error bars represent their standard deviation for the 20 sub-appertures. For the overcast day on the Figure 1, the coherence time of the intensity, taking into account the standard deviation, varies between 20 ms and 55 ms. And for the

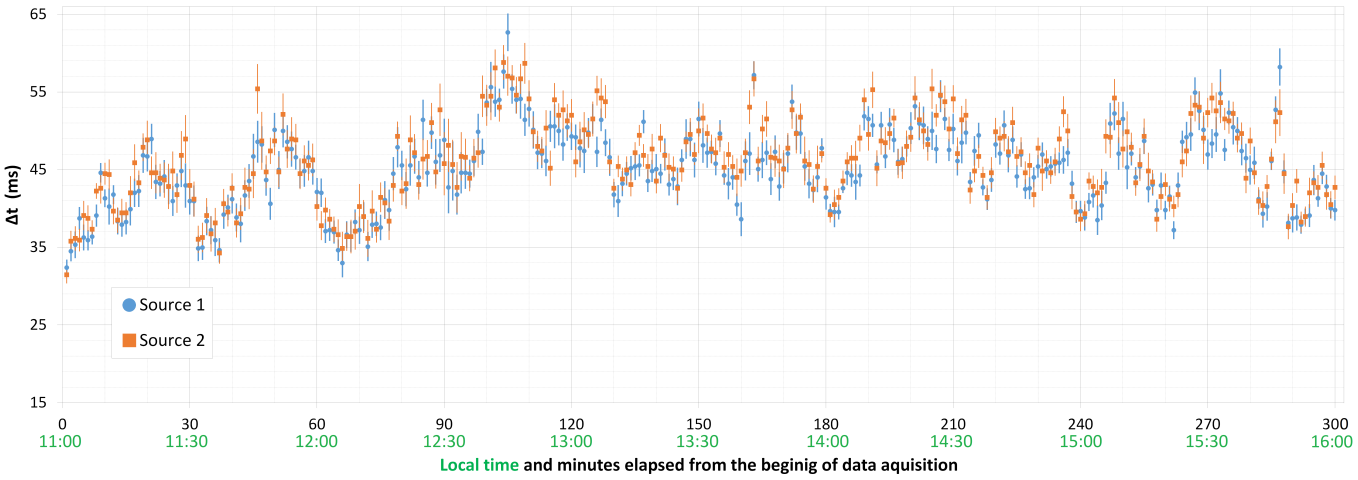

Figure 2. Temporal evolution of the coherence time (Δt) for each source with its standard deviation (October 30$^{\text{th}}$, 2015).

sunny day in Figure 2, the coherence time of the intensity varies from 30 ms to 65 ms. The evolution of the channel is much slower than telecom symbol duration time for few Gbit/s, for instant the symbol duration time is around 0.33 ns for 3 Gbit/s. So for a FSO link using direct detection (power in the bucket) the channel is stationary during several million of bits. But if the signal falls under the detection threshold the blackout lasts also several tenths of ms [8]. This long fading duration needs to be mitigated with numerical techniques such as coding and data interleaving in order to make the information re-transmitted.

For these two days, with a varing visibility and solar enlightenment conditions, the order of magnitude of the coherence time of the intensity are similar. On the other hand their standard deviation is larger for the October 30$^{\text{th}}$. This does not come from a difference of the turbulence strength, since the Fried diameter is 30 cm and 31 cm for October 19$^{\text{th}}$ and October 30$^{\text{th}}$ respectively. The Fried diameter corresponds to the equivalent diameter of an infinite diameter telescope which would be limited by turbulence. In other words, is the total amount of turbulence along the line of sight by integrating the C_n^2 profile.

The enhanced spread of the intensity coherence times among the sub-channels on October, 30$^{\text{th}}$ could be due to the direction of the wind. On October 19$^{\text{th}}$, the wind is perpendicular to the line of sight. That induces turbulence cells moving in front of the sub-apertures. Therefore all sub-apertures are imaging the same portion of the turbulence cell, which went in front of the full aperture in $D_{telescope}/|v_0| = 0.35/2.5 = 140$ ms. That is why the values of coherence time for each sub channels are very close from one another. On the October 30$^{\text{th}}$, the wind was parallel to the line of sight so in this case each sub aperture is imaging different parts of the turbulence cell that is why the values of coherence time of the intensity are more spread on this day.

2.3 Coherence time of the phase

The goal of this investigation is to determine the Greenwood frequency f_G which corresponds to the optimal frequency required for the correction of an AO system. The AO system helps to stabilize the laser beam (i.e beam wander). In fact the beam stabilization is necessary to coupling the beam into a fiber or a detector and reduce fading. For our experimentation we focus on the coherence time of the phase τ_0 which is linked to Greenwood frequency by this equation [9]:

$$f_G = 0.134\tau_0^{-1} \tag{3}$$

And the coherence time of phase can be computed with the following equation [10]:

$$\tau_0 = 0.314 \, \frac{r_0}{v_0} \, . \tag{4}$$

The r_0 represents the Fried diameter [11] and the v_0 is the perpendicular component to the line of sight of the wind speed. On October, 19$^{\text{th}}$ the wind perpendicular to the line of sight that is why we chose to study this day where v_0 is equal to 2.5 m/s. The coherence time of the phase is computed from the temporal evolution of the Fried diameter, which is derived from variances of the wave-front slopes. Ultimately we estimate the coherence time of the phase τ_0 by using the long term slopes time series recorded together with the intensity series. The slopes time series are gathered in 1 minutes packets, the slope variances of each packet are computed and the variances are used to determine the Fried diameter according to [12]:

$$r_0 = \varnothing_{\text{subap.}} \left(4 \left(\frac{1}{f_{\text{sampl.}}} \right)^2 \frac{0.16}{var_{\text{xy}}} \right)^{(3/5)}, \tag{5}$$

where $\varnothing_{\text{subap.}}$ is the diameter of a sub-aperture, here 7 cm; $f_{\text{sampl.}}$ the subsampling factor equals to 2 for our Shack-Hartmann wave-front sensor and var_{xy} the slope variances (in pixel×pixel).

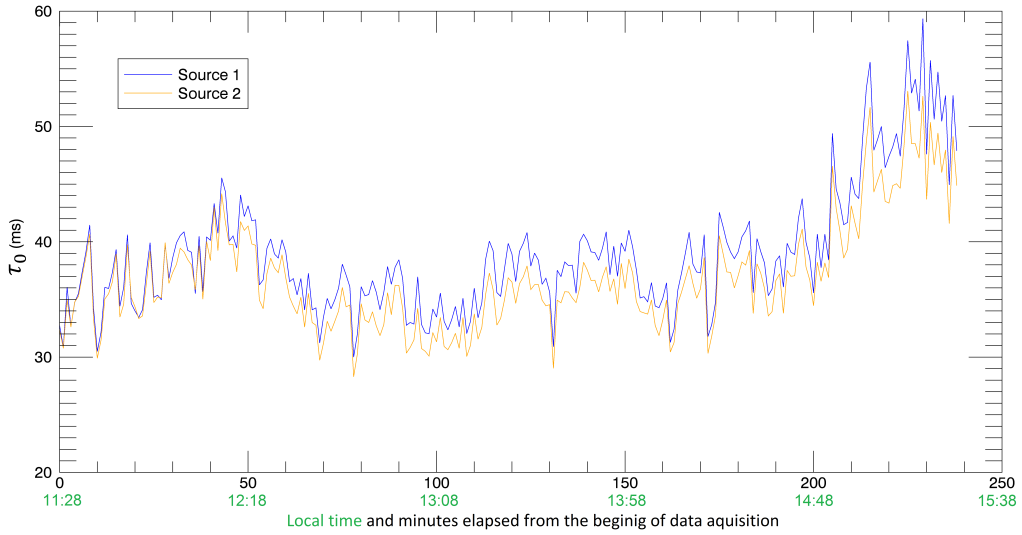

Figure 3. Temporal evolution of the coherence time of the phase τ_0 for each source (October 19$^{\text{th}}$, 2015).

On the Figure 3 we can observe the evolution of the coherence time of phase for each sources. It varies between 28 ms and 60 ms and is directly proportional to the r_0 in accordance to Equation 4. Around midday, turbulence is stronger than later in the afternoon when the τ_0 increases with r_0. These large values corresponding to a Grennwood frequency of 2.2-4.8 Hz, mean that the beam wander will be easy stabilized for adaptive optics system using.

Nevertheless, the coherence time of the phase for an horizontal propagation channel close to ground is ten times higher than for a ground to space channel, with a typical value of 5 ms [10]. This difference comes from two effects. The first one comes from the proportionality of the coherence time with r_0 so τ_0 proportional at $\lambda^{6/5}$. Therefore for an equal strong of turbulence at the ground, the change of $\lambda = 4$ μm in $\lambda = 1.55$ μm induces a decrease of a factor 3 on the coherence time of phase. The second effect comes from the difference of line of sight. The horizontal path crosses quasi constant values of C_n^2 near ground and a slant path from ground to space takes into account a fast decreasing C_n^2 with height on the first km (about of one order of magnitude). Hence despite the larger decorrelation of the phase in the horizontal case, we conclude the wavelength has a preponderant effect against the line of sight.

The correlation of the values of the coherence time of the phase and of the intensity is computed, reveals a weak correlation of -36% for source 1 and -27% for source 2. This is due to the fact that they are affected by the turbulent wavefront at different places along the line of sight. The coherence time of the phase which depends on Fried diameter brings information on the turbulence near the wave-front sensor and the coherence time of the

intensity bring information on turbulence variation in the middle of the line of sight [13]. In fact for an horizontal sight-line the C_n^2 are inhomogeneous. To investigate the details on these inhomogeneities along the line of sight, a distributed profile of the structure constant of refractive index fluctuations $C_n^2(z)$, which represents the strength of turbulence, has to be estimated [14].

3. CONCLUSIONS AND PROSPECTS

In this paper we have described the SCINDAR, our experimental instrument which characterized the channel. And finally we presented and discussed the results of the coherence time of the intensity and the phase, which are computed with our experimental data.

The coherence time of the intensity for a 40-m high horizontal link is equal to several tenths of ms, higher than the telecom symbol duration time for few Gbit/s, so the channel is stationary during several millions of bits. But when the signal falls under the detection threshold a smart numerical coding and interleaving will be necessary to transmit again. At last the coherence time of the phase is found to be equal to several dozen of ms. That enables the use of adaptive optics components in order to increase the flux coupled to the receiver and so improve the signal. The urban low height horizontal atmospheric channel we characterized in this paper has slow evolution constants. So there is no show stopper to design a horizontal FSO link at 4 μm, with available laser source and detector at 4 μm.

We plan an experiment with the modified SCINDAR in order to receive the telecom signal and characterize the channel in the same time. This simultaneous diagnostic will bring accurate information of the impact of a real channel conditions occuring on the communication link. It will give us the chance to build a new turbulence database consequently. The diversity in terms of weather conditions of our data base will allow the study of the interaction between the wind, the turbulence and the coherence times of the intensity.

REFERENCES

[1] Khalighi, M. A. and Uysal, M., "Survey on Free Space Optical Communication: A Communication Theory Perspective," *IEEE Communications Surveys Tutorials* **16**(4), 2231–2258 (2014).

[2] Esmail, M. A., Fathallah, H., and Alouini, M. S., "Outdoor FSO Communications Under Fog: Attenuation Modeling and Performance Evaluation," *IEEE Photonics Journal* **8**, 1–22 (Aug. 2016).

[3] Stotts, L. B., Stadler, B., Hughes, D., Kolodzy, P., Pike, A., Young, D. W., Sluz, J., Juarez, J., Graves, B., Dougherty, D., Douglass, J., and Martin, T., "Optical communications in atmospheric turbulence," **7464**, 746403, International Society for Optics and Photonics (Aug. 2009).

[4] Sauvage, C., Robert, C., Sorrente, B., Grillot, F., and Erasme, D., "Study of short and mid-wavelength infrared telecom links performance for different climatic conditions," in [*Environmental Effects on Light Propagation and Adaptive Systems II*], **11153**, 111530I, International Society for Optics and Photonics (Nov. 2019).

[5] "MATISSE-V3.0 | Matisse." https://matisse.onera.fr/en.

[6] Nguyen, K.-L., Robert, C., Cohard, J. M., Lagouarde, J.-P., Irvine, M., Conan, J.-M., and Mugnier, L. M., "Measurement of the spatial distribution of atmospheric turbulence with SCINDAR on a mosaic of urban surfaces," **10425**, 104250L, International Society for Optics and Photonics (Oct. 2017).

[7] Pang, X., Ozolins, O., Schatz, R., Storck, J., Udalcovs, A., Navarro, J. R., Kakkar, A., Maisons, G., Carras, M., Jacobsen, G., Popov, S., and Lourdudoss, S., "Gigabit free-space multi-level signal transmission with a mid-infrared quantum cascade laser operating at room temperature," *Optics Letters* **42**, 3646–3649 (Sept. 2017).

[8] Sauvage, C., Robert, C., Sorrente, B., and Erasme, D., "Temporal characterization of an urban horizontal atmospheric telecom channel," in [*Imaging and Applied Optics 2019 (COSI, IS, MATH, pcAOP)*], PW4C.5, OSA, Munich (2019).

[9] Fried, D. L., "Time-delay-induced mean-square error in adaptive optics," *Journal of the Optical Society of America A* **7**, 1224 (July 1990).

[10] García-Lorenzo, B., Eff-Darwich, A., Fuensalida, J. J., and Castro-Almazán, J., "Adaptive optics parameters connection to wind speed at the Teide Observatory," *Monthly Notices of the Royal Astronomical Society* **397**, 1633–1646 (Aug. 2009).

[11] Fried, D. L., "Limiting Resolution Looking Down Through the Atmosphere," *JOSA* **56**, 1380–1384 (Oct. 1966). Publisher: Optical Society of America.

[12] Noël, T., *Caracterisation spatiale et temporelle de la turbulence atmospherique par analyse de front d'onde*, these de doctorat, Paris 6 (Jan. 1997).

[13] Sauvage, C., Robert, C., Mugnier, L., Conan, J.-M., Cohard, J. M., Nguyen, K. L., Irvine, M., and Lagouarde, J.-P., "Near ground horizontal high resolution C_n^2 profiling from Shack Hartmann slopes and scintillation data," *To be submited in Boundary Layer Meteorology* .

[14] Robert, C., Velluet, M.-T., Masciadri, E., Turchi, A., Conan, J.-M., Védrenne, N., Artaud, G., and Benammar, B., "Characterization of the turbulent atmospheric channel of space-ground optical links with parametric models: description and cross-validation with mesoscale models and in situ measurements," in [*Environmental Effects on Light Propagation and Adaptive Systems II*], **11153**, 1115304, International Society for Optics and Photonics (Oct. 2019).